Surface properties of the half-and full-Heusler alloys

2002 J. Phys.: Condens. Matter 14 6329

(http://iopscience.iop.org/0953-8984/14/25/303)

INSTITUTE OF PHYSICS PUBLISHING JOURNAL OF PHYSICS: CONDENSED MATTER

J. Phys.: Condens. Matter **14** (2002) 6329–6340 PII: S0953-8984(02)35615-7

Surface properties of the half- and full-Heusler alloys

I Galanakis[1]

Institut für Festkörperforschung, Forschungszentrum Jülich, D-52425 Jülich, Germany

E-mail: I.Galanakis@fz-juelich.de

Received 8 April 2002
Published 14 June 2002
Online at stacks.iop.org/JPhysCM/14/6329

Abstract

Using a full-potential *ab initio* technique I study the electronic and magnetic properties of the (001) surfaces of the half-Heusler alloys NiMnSb, CoMnSb and PtMnSb and of the full-Heusler alloys Co_2MnGe, Co_2MnSi and Co_2CrAl. The MnSb-terminated surfaces of the half-Heusler compounds present properties similar to those of the bulk compounds and, although the half-metallicity is lost, an important spin polarization at the Fermi level. In contrast to this, the Ni-terminated surface shows an almost zero net spin polarization. While the bulk Co_2MnGe and Co_2MnSi are almost half-ferromagnetic, their surfaces lose the half-metallic character and the net spin polarization at the Fermi level is close to zero. In contrast, the CrAl-terminated (001) surface of Co_2CrAl shows a spin polarization of about 84%.

1. Introduction

Since the discovery of giant magnetoresistance (GMR) by the groups of Fert [1] and Grünberg [2] in 1988, a new field in condensed matter, magnetoelectronics or spin electronics, has evolved and grown steadily in the last ten years. One of the most interesting problems of this new field is the spin injection from a ferromagnet into a semiconductor, which should lead to the creation of efficient spin filters [3], tunnel junctions [4], GMR devices for spin injection [5] etc. This has intensified the interest in the so-called half-ferromagnetic materials which have a band gap at the Fermi level (E_F) for one spin direction and thus exhibit 100% spin polarization at E_F. So, in principle, during the spin-injection process only spin-up electrons should be injected into the semiconductor, allowing the creation of the perfect spin filter and spin-dependent devices with superior performances.

The Heusler alloys are attractive candidates for providing half-ferromagnetic materials; there are two distinct families of these. The compounds of the first family have the form XYZ and crystallize in the $C1_b$ structure, which consists of four fcc sublattices occupied by the three atoms X, Y and Z and a vacant site [6]. They are also known as half-Heusler

[1] Author to whom any correspondence should be addressed.

compounds. In 1983 de Groot and collaborators [7] showed that one of them, NiMnSb, has a gap at E_F in the minority band. Also PtMnSb [8, 9] and CoMnSb [10] have been predicted to be half-ferromagnets. Infrared absorption [11] and spin-polarized positron-annihilation [12] experiments have verified the half-ferromagnetic character of bulk NiMnSb. There is also ellipsometric evidence of the spin-down gap for PtMnSb [13].

Recently it has become possible to grow high-quality films of Heusler alloys and it is mainly NiMnSb that has attracted the attention [14]. Unfortunately these films were found not to be half-ferromagnetic [15–18]; a maximum value of 58% for the spin polarization of NiMnSb was obtained by Soulen *et al* [15]. These polarization values are consistent with a small perpendicular magnetoresistance measured for NiMnSb in a spin-valve structure [19], a superconducting tunnel junction [4] and a tunnel magnetoresistive junction [20]. Ristoiu *et al* [21] showed that during the growth of the NiMnSb thin films, Sb and then Mn atoms segregate to the surface, which is far from being perfect, thus decreasing the spin polarization obtained. But when they removed the excess of Sb by a flash annealing, they managed to get a nearly stoichiometric ordered alloy surface terminated by a MnSb layer, which presented a spin polarization of about $67 \pm 9\%$ at room temperature [21]. The temperature dependence of the spin moments for such a film was studied by Borca *et al* [22]. Wijs and de Groot [23] have shown by first-principles calculations that NiMnSb surfaces do not present 100% spin polarization and they proposed that at some interfaces it is possible to restore the half-ferromagnetic character of NiMnSb. Also recently, Jenkins and King studied by a pseudopotential technique the MnSb-terminated (001) surface of NiMnSb and showed that there are two surface states at the Fermi level, which are well localized at the surface layer [24] and persist even when the MnSb surface is covered by an Sb overlayer [25]. They found also that the surface only mildly reconstructs; the Sb atoms move outwards, the Mn atoms inwards with a total buckling of only 0.06 Å and this small $c(1 \times 1)$ reconstruction is energetically more favourable than the creation of Mn or Sb dimers.

The second family of Heusler alloys are the so-called full-Heusler alloys and they have the X_2YZ formula. They crystallize in the $L2_1$ structure which is similar to the $C1_b$ structure but now the vacant site is occupied by an X atom. They have attracted a lot of attention due to the diverse magnetic phenomena they present [6, 26] and mainly the transition from a ferromagnetic phase to an antiferromagnetic one obtained by changing the concentration of the carriers [27]. Webster [28] was the first to synthesize full-Heusler alloys containing Co, and Ishida and collaborators [29] have proposed that the compounds of the type Co_2MnZ, where Z stands for Si and Ge, are also half-ferromagnets. But Brown *et al* [30] using polarized neutron diffraction measurements have shown that there is a finite very small spin-down DOS at the Fermi level instead of an absolute gap. Recently, Ambrose *et al* [31] managed to grow a Co_2MnGe thin film on a GaAs(001) substrate by molecular beam epitaxy, and Geiersbach *et al* [32] grew by sputtering (110) thin films of Co_2MnSi, Co_2MnGe and Co_2MnSn using a metallic seed on top of a MgO(001) substrate.

In this communication I study the (001) surfaces of the NiMnSb, CoMnSb and PtMnSb half-ferromagnetic materials taking into account the two different possible terminations. I compare their magnetic and electronic properties with the bulk calculations and can explain the large spin polarization obtained for the MnSb-terminated (001) surface of NiMnSb. The second part of my study is devoted to the (001) surfaces of the Co_2MnGe and Co_2CrAl compounds. The substitution of Cr for Mn leads to a change in the electronic properties of the surfaces studied and the CrAl-terminated surfaces show very large spin polarizations of about 84%.

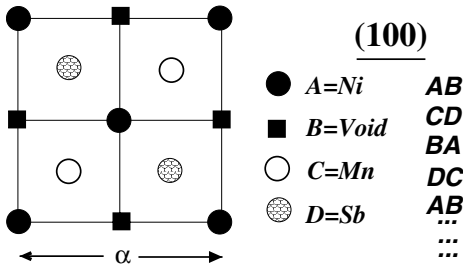

Figure 1. A schematic representation of the (001) surface of NiMnSb. There are two possible terminations: (i) MnSb and (ii) Ni/vacancy. The interlayer distance is 0.25 a. In the $i \pm 2$ layer the atoms have exchanged positions compared to those in layer i. In the case of the Co_2MnGe compound the Co atoms occupy the Ni and vacant sites.

2. Method

In the calculations I used the full-potential version of the screened Korringa–Kohn–Rostoker (KKR) Green function method [33, 34] in conjunction with the local spin-density approximation [35]. The full potential is implemented by using a Voronoi construction of Wigner–Seitz polyhedra that fill the space [34]. To simulate the surface I used a slab with 15 metal layers embedded in a half-infinite vacuum from each side. Such a slab has two equivalent surfaces, avoiding the creation of slab dipoles. This slab thickness is sufficient for the layers in the middle to exhibit bulk properties; they show a spin-down gap of the same width as in the bulk and the same relative position of the Fermi level and finally the magnetic moments differ by $<0.01\ \mu_B$ from the bulk values. I have also converged the $\boldsymbol{q}_\parallel$-space grid, the number of energy points and the tight-binding cluster so that the properties of the surfaces do not change (similar DOS and spin moments). So I have used a two-dimensional 30×30 $\boldsymbol{q}_\parallel$-space grid to perform the integrations in the first surface Brillouin zone. To evaluate the charge density one has to integrate the Green function over an energy contour in the complex energy plane; for this, 42 energy points were needed. A tight-binding cluster of 51 atoms was used in the calculation of the screened KKR structure constants [36]. Finally, for the wavefunctions I took angular momentum up to $\ell_{max} = 3$ into account and for the charge density up to $\ell_{max} = 6$.

In figure 1 I present the structure of the (001) surfaces in the case of NiMnSb. There are two different possible terminations, one containing the Mn and Sb atoms while the other contains the Ni atom and the vacant site. In the case of the full-Heusler alloys such as Co_2MnGe, there are also two possible surface terminations: the first one containing the Mn and Ge atoms in the surface layer while the second one is Co terminated (in figure 1 both the vacant and Ni sites are occupied by Co atoms). The interlayer distance is 0.25 times the lattice constant. I have used in all my calculations the experimental lattice constants [6]. In the perpendicular direction the layer occupancy is repeated every fourth layer, since in the $i \pm 2$ layer the atoms have exchanged positions compared to those in layer i.

3. Half-Heusler alloys

3.1. Density of states

In the first part of my study I concentrate on the half-Heusler compounds and more specifically on the (001) surfaces of NiMnSb, CoMnSb and PtMnSb. I use the NiMnSb compound as the model system and at the end of the section I discuss its differences from the other two alloys. As

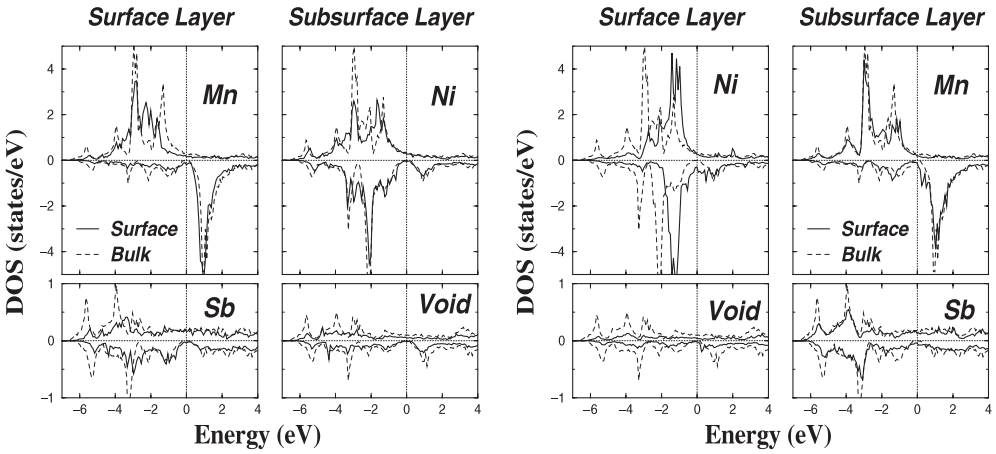

Figure 2. Spin- and atom-projected DOS for the MnSb-terminated NiMnSb(001) surface (left panel) and for the Ni/vacancy-terminated (001) surface (right panel). The dashed curves give the local DOS of the atoms in the bulk.

already discussed in the introduction, the MnSb-terminated surface of NiMnSb shows a very small reconstruction, while no information is available for the Ni-terminated surface which in principle should show a large reconstruction due to the vacant site at the surface. In my study I assume an 'ideal' epitaxy in both cases. In the left panel of figure 2 I present the atom- and spin-projected densities of states (DOS) for the Mn and Sb atoms in the surface layer and the Ni and vacant sites in the subsurface layer for the MnSb-terminated NiMnSb(001) surface, and in the right panel of the same figure I present the atom- and spin-projected DOS of the surface and the subsurface layers for the Ni-terminated surface. In both cases I compare the surface DOS with the bulk calculations (dashed curve) [37].

In the case of the MnSb-terminated surface, the DOS with the exception of the gap area is very similar to the bulk calculations. The Ni atom in the subsurface layer presents practically a half-ferromagnetic character with an almost zero spin-down DOS, while for the bulk there is an absolute gap. The spin-down band of the vacant site also presents a very small DOS around the Fermi level. The Mn and Sb atoms in the surface layer show more pronounced differences with respect to the bulk, and within the gap there are very small Mn d and Sb p DOS. These states are strongly localized at the surface layer, as at the subsurface layer there are practically no states inside the gap. This is in agreement with previous pseudopotential calculations that showed that the surface states in the case of the MnSb-terminated NiMnSb(001) surface are localized at the surface layer [24]. Our results are in agreement with the experiments of Ristoiu *et al* [21] who in the case of a MnSb well ordered (001) surface measured a high spin polarization.

3.2. Magnetic moments

In table 1 I have gathered the spin magnetic moments of the atoms in the surface and subsurface layers. In the case of the MnSb-terminated NiMnSb(001) surface, the Ni and vacant sites at the subsurface layer gain a similar charge to in the case of the bulk, $\sim 0.5e^-$ for Ni and $\sim 1.3e^-$ for the vacant site. Also the Ni and vacant spin moments are comparable to those in the bulk situation. The Mn in the surface layer loses $\sim 0.3e^-$ more than the bulk Mn and the Sb atom also loses $\sim 0.1e^-$ more, due to the spilling out of charge into the vacuum. The spin magnetic moment of the Mn atom in the surface layer increases with respect to the bulk and reaches

Table 1. Spin moments in μ_B for the NiMnSb, PtMnSb and CoMnSb compounds in the case of: (i) bulk compounds; (ii) the Mn and Sb atoms in the surface and the Ni (Pt, Co) and the vacant site in the subsurface layer for the MnSb-terminated (001) surfaces; (iii) the same as (ii) but for the Ni-, Pt- or Co-terminated surfaces. For the surfaces the 'total' moment denotes the sum of the moments in the surface and subsurface layers.

m^{spin} (μ_B)		Ni (Pt, Co)	Mn	Sb	Vacancy	Total
NiMnSb	Bulk	0.26	3.70	−0.06	0.05	3.96
	(001)MnSb	0.22	4.02	−0.10	0.04	4.19
	(001)Ni	0.46	3.84	−0.05	0.05	4.30
PtMnSb	Bulk	0.09	3.89	−0.08	0.04	3.94
	(001)MnSb	0.08	4.19	−0.13	0.03	4.17
	(001)Pt	0.27	4.15	−0.04	0.04	4.42
CoMnSb	Bulk	−0.13	3.18	−0.10	0.01	2.96
	(001)MnSb	−0.06	3.83	−0.12	0.01	3.65
	(001)Co	1.19	3.31	−0.09	0.02	4.43

$\sim 4\ \mu_B$. This behaviour arises from the reduced symmetry of the Mn atom in the surface which loses two of the four neighbouring Co atoms. In the majority band this leads to a narrowing of the d DOS and a slight increase of the d count by $0.10e^-$ due to rehybridization, while in the minority valence band the Mn d contribution is decreased by $0.20e^-$. Moreover the splitting between the unoccupied Mn states above E_F and the centre of the occupied Mn states decreases and at E_F a surface states appears. I should also mention here that in the case of a half-ferromagnetic material the total spin magnetic moment per unit cell should be an integer since the total number of valence electrons and the number of spin-down occupied states are integers; the spin moment in μ_B is simply the number of uncompensated spins. The total spin moment for the NiMnSb compound is 4 μ_B (note that in the KKR method one can get the correct charge only if Lloyd's formula is used for the evaluation of the charge density. Otherwise, as is the case in these calculations, the finite-ℓ cut-off results in small numerical inaccuracies). Thus in the case of the surfaces the half-ferromagnetic character is lost and an increase of the total spin moment is observed, which is no longer an integer.

In the case of the Ni-terminated surface, the changes in the DOS compared to the bulk one are more pronounced. The Ni atom in the surface instead of gaining $\sim 0.5e^-$ as in the bulk now loses $\sim 0.15e^-$. Also the vacant site gains only half of the charge that it gains in the bulk. Due to charge neutrality the Ni d bands move higher in energy. As was the case for the Mn surface atom in the MnSb-terminated surface, the Ni spin magnetic moment is increased (see table 1). The Mn and Sb atoms in the subsurface layer present a charge transfer comparable to that in the bulk compound and also a comparable spin moment. Within the gap there are small Sb and Mn DOS of comparable intensity to those of the Mn and Sb atoms at the surface layer of the MnSb-terminated surface. Deeper than the third layer from the surface, the atoms regain a bulk-like behaviour. The origins of the surface states are not the same for the two different terminations. In the case of the Ni-terminated surface there is a practically rigid shift (although also the shapes of the peaks and their intensities change) towards higher energies of the Ni bands and now the Fermi level crosses a region of high DOS for both spin directions. In the case of the MnSb-terminated surface, the DOS of the Mn atom at the surface is very similar to the bulk case. The small spin-down DOS inside the gap comes from a d-like atomic state of Mn that is shifted with respect to the continuum due to the lower symmetry of the surface. This peak is broadened by the interaction of the Mn atom with its neighbours, finally forming a surface band within the gap. This state is not localized only at the Mn atom but extends also to the Sb neighbouring atoms as electrons are delocalized in the two dimensions.

The Ni atoms at the subsurface are slightly polarized by the Mn atoms and show a very small DOS within the gap.

3.3. Spin polarization

As discussed in the previous paragraph, the main difference in surface DOS between the two terminations is the different origins of the surface states. This behaviour is also reflected in the spin polarization of the surfaces. In table 2 I have gathered the number of spin-up and spin-down states at the Fermi level for each atom at the surface and the subsurface layer for both terminations. I calculated the spin polarization as the ratio of the number of spin-up states minus the number of spin-down states to the total DOS at the Fermi level. P_1 corresponds to the spin polarization when I take into account only the surface layer and P_2 when I also include the subsurface layer. P_2 represents the experimental situation quite well, as the spin polarization in the case of films is usually measured using inverse photoemission which probes only the surface of the sample [38]. In all cases the inclusion of the subsurface layer increased the spin polarization. In the case of the Ni-terminated surface, the spin-up DOS at the Fermi level is equal to the spin-down DOS and the net polarization P_2 is zero. In the case of the MnSb-terminated surface the spin polarization increases and now P_2 reaches a value of 38%, which means that the spin-up DOS at the Fermi level is about two times the spin-down DOS. As can be seen in table 2 the main difference between the cases for the two different terminations is in the contribution of the Ni spin-down states. In the case of the MnSb surface the Ni in the subsurface layer has a spin-down DOS at the Fermi level of 0.05 states eV^{-1}, while in the case of the Ni-terminated surface the Ni spin-down DOS at the Fermi level is 0.40 states eV^{-1}, considerably decreasing the spin polarization for the Ni-terminated surface; the Ni spin-up DOS are the same for the two terminations. It is interesting also to note that for both surfaces the net Mn spin polarization is close to zero while Sb atoms in both cases show a large spin polarization and the number of the Sb spin-up states is similar to the number of Mn spin-up states; thus Sb and not Mn is responsible for the large spin polarization of the MnSb layer in both surface terminations. The calculated P_2-value of 38% for the MnSb-terminated surface is smaller than the experimental value of 67% obtained by Ristoiu and collaborators [21] for a thin film terminated in a MnSb stoichiometric alloy surface layer. But experimentally no exact details of the structure of the film are known and the comparison between experiment and theory is not straightforward.

3.4. CoMnSb(001) and PtMnSb(001)

In figure 3 I present the spin-resolved DOS for the Co and Mn atoms in the case of the two differently terminated CoMnSb(001) surfaces and the Pt and Mn DOS for the PtMnSb surfaces. Both CoMnSb and PtMnSb present a behaviour similar to that of the NiMnSb surfaces. In the case of the MnSb-terminated surfaces the DOS of the Co or Pt atom in the subsurface layer is similar to the bulk one and so is the charge transfer. The Mn and Sb atoms at the surface—as was the case for the MnSb-terminated NiMnSb(001) surface—show small DOS within the gap and these states are localized at the surface layer. The atom-resolved spin moments are also close to the bulk values (see table 1) but the total spin magnetic moment is no longer an integer, reflecting the loss of the half-metallicity for the surfaces. As was the case for the Ni-terminated surface, the spin magnetic moments of the Co and Pt atoms in the case of the Pt- and Co-terminated surfaces, respectively, increase considerably with respect to the bulk. The Mn and Sb atoms at the subsurface layer are close to showing the bulk behaviour exactly, as was the case for the Ni-terminated surface. It is also interesting to examine the spin polarization at the Fermi level. In

Table 2. Atom-resolved spin-up and spin-down DOS at the Fermi level in states eV^{-1}. They are presented as spin-up over spin-down ratios. Polarization ratios at the Fermi level are calculated taking into account only the surface layer, P_1, and both the surface and subsurface layers, P_2.

	MnSb termination					
	Surface layer		Subsurface layer		P_1 ($\frac{\uparrow-\downarrow}{\uparrow+\downarrow}$)	P_2 ($\frac{\uparrow-\downarrow}{\uparrow+\downarrow}$)
	Mn (↑/↓)	Sb (↑/↓)	Ni (Co, Pt) (↑/↓)	Vacancy (↑/↓)	(%)	(%)
NiMnSb	0.16/0.19	0.17/0.03	0.28/0.05	0.05/0.02	26	38
CoMnSb	0.23/0.27	0.16/0.07	0.91/0.15	0.07/0.02	6	46
PtMnSb	0.21/0.24	0.31/0.06	0.38/0.04	0.08/0.02	26	46
	Ni (Co, Pt)/vacancy termination					
	Subsurface layer		Surface layer		P_1 ($\frac{\uparrow-\downarrow}{\uparrow+\downarrow}$)	P_2 ($\frac{\uparrow-\downarrow}{\uparrow+\downarrow}$)
	Mn (↑/↓)	Sb (↑/↓)	Ni (Co, Pt) (↑/↓)	Vacancy (↑/↓)	(%)	(%)
NiMnSb	0.18/0.16	0.13/0.05	0.27/0.40	0.04/0.02	−16	0
CoMnSb	0.55/0.68	0.12/0.07	0.54/1.15	0.05/0.04	−34	−22
PtMnSb	0.18/0.14	0.21/0.07	0.30/0.24	0.05/0.02	14	22

the case of the Co-terminated CoMnSb surface, as was the case for the Ni-terminated surface, there is a shift of the Co spin-down DOS towards higher energies and the Co spin-down DOS at the Fermi level is very high and thus P_2 is negative, meaning that the spin-down DOS is larger than the spin-up DOS at the Fermi level. In the case of the MnSb-terminated CoMnSb surface, the Co atom in the subsurface layer has practically zero spin-down DOS and P_2 reaches 46%. In the case of PtMnSb, Pt does not show such a pronounced difference between its behaviours for the two surface terminations as the Co atom, because it has practically all its d states filled and the DOS near the Fermi level is small. But for PtMnSb also, the MnSb-terminated surface shows a very large spin polarization comparable to that for CoMnSb, while the Pt-terminated (001) surface shows a positive spin polarization in contrast to the vanishing net spin polarization of the Ni surface and the negative one of the Co-terminated surface.

4. Full-Heusler alloys

In the second part of my study I concentrate on the surface properties of the full-Heusler alloys containing Co. I have made calculations for the Co_2MnGe, Co_2MnSi and Co_2CrAl compounds. Ge and Si are isoelectronic elements and thus Co_2MnGe and Co_2MnSi present similar properties both as bulk systems and as surfaces (they present similar magnetic moments, as can be seen in table 3, and similar DOS) and therefore I only discuss the properties of Co_2MnGe. The interest in Co_2MnGe arises mainly from the fact that it is the only full-Heusler alloy that has been grown on a semiconductor [31]. Co_2MnSi has the same experimental lattice constant as GaAs and AlAs [6] and Co_2CrAl presents a very large spin-up DOS at the Fermi level due to the smaller exchange splitting of the Cr d states compared to the Mn d states. Our calculations show that the bulk compounds are half-ferromagnets with only a tiny gap—contrary to the indications of the early calculations of Ishida *et al* [29] using the linear muffin-tin orbital (LMTO) method in the atomic sphere approximation, and the Fermi level falls within a broad region of finite very small spin-down DOS. The highest occupied bands and the lowest unoccupied bands touch the Fermi level, destroying the indirect gap [39]. These results agree with the experimental results of Brown and collaborators [30] who, using

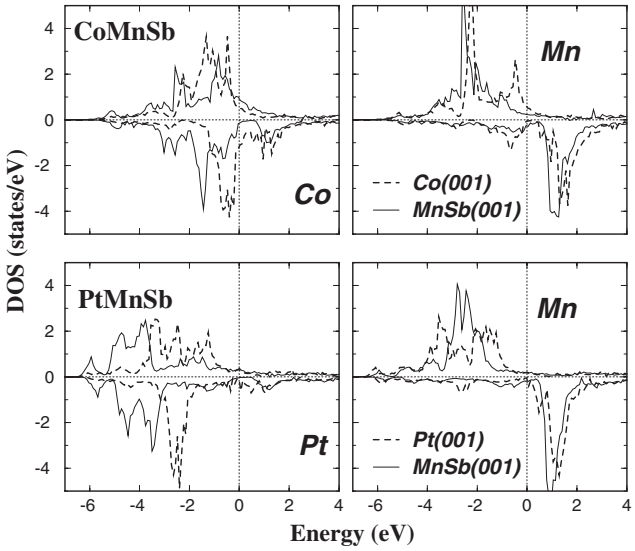

Figure 3. In the upper panel the spin-resolved DOS for Co in the surface layer and Mn in the subsurface layer in the case of the Co-terminated CoMnSb(001) surface and for Co in the subsurface layer and Mn in the surface layer for an MnSb-terminated CoMnSb(001) surface. In the bottom panel the spin-resolved DOS of the PtMnSb surface for the Pt and MnSb terminations are given.

Table 3. Spin moments in μ_B for the Co_2MnGe, Co_2MnSi and Co_2CrAl compounds in the case of: (i) bulk compounds; (ii) the Mn (Cr) and Ge (Si, Al) atoms in the surface and the Co atoms in the subsurface layer for the MnGe- (MnSi-, CrAl-) terminated (001) surfaces; (iii) the same as (ii) but for the Co-terminated surfaces. For the surfaces the 'total' moment denotes the sum of the moments in the surface and subsurface layers.

m^{spin} (μ_B)		Co	Mn (Cr)	Ge (Si, Al)	Total
Co_2MnGe	Bulk	0.98	3.04	−0.06	4.94
	(001)MnGe	0.96	3.65	−0.10	5.47
	(001)Co	1.40	2.85	−0.09	5.56
Co_2MnSi	Bulk	1.02	2.97	−0.07	4.94
	(001)MnSi	0.95	3.56	−0.13	5.33
	(001)Co	1.29	2.72	−0.11	5.19
Co_2CrAl	Bulk	0.76	1.54	−0.10	2.96
	(001)CrAl	0.76	3.12	−0.02	4.62
	(001)Co	1.36	1.06	−0.11	3.67

polarized neutron diffraction measurements, have shown that there is a finite, but very small, DOS at the Fermi level instead of an absolute gap.

4.1. Co-terminated surfaces

In table 3 I present the spin magnetic moments for the full-Heusler alloys under study and in figure 4 the Co and Mn (Cr) DOS for the two possible terminations for the Co_2MnGe (left panel) and Co_2CrAl (right panel) compounds. I compare in all cases the surface DOS with the bulk DOS (dashed curves). In the case of the Co-terminated surfaces the two compounds show the same behaviour, which is similar to the behaviour of the Co surface atom in the case of the Co-terminated CoMnSb surface. The lower coordination number of the Co atoms in the

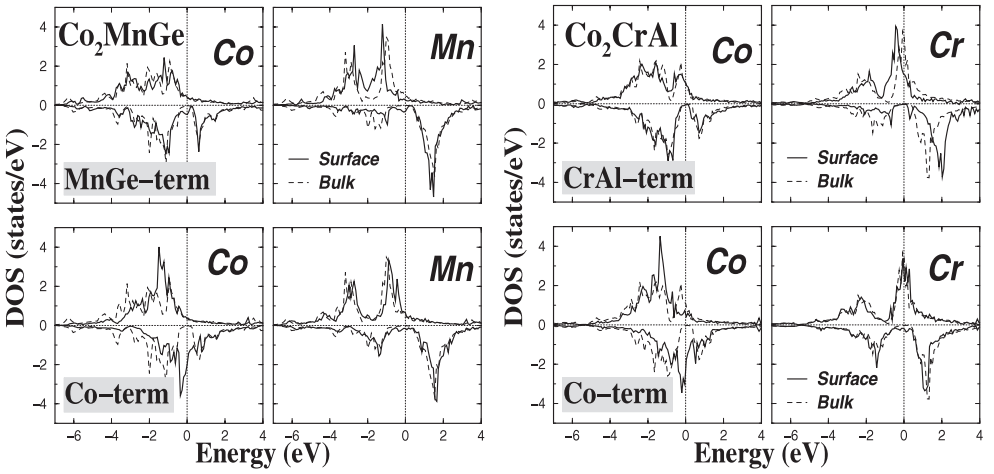

Figure 4. Atom- and spin-projected DOS for the Mn atom in the surface and the Co atom in the subsurface layer in the case of the MnGe-terminated $Co_2MnGe(001)$ surface (upper left panel) and the Co atom in the surface layer and the Mn atom in the subsurface for the Co-terminated surface (bottom left panel). In the right panel the similar DOS for the Co_2CrAl compound is shown. The dashed curve shows the bulk results.

surface layer results in smaller covalent hybridization between the Co spin-down d states and the Mn ones and thus there is a practically rigid shift of the spin-down Co d bands towards higher energies, and now the Fermi level falls at the edge of the large peak of the minority-spin DOS. Due to this large peak it is very likely that this surface would reconstruct. The Mn and Cr atoms in the subsurface layer show now a considerable spin-down DOS within the pseudogap due to the hybridization with the spin-down d states of the surface Co atoms. As was the case for the CoMnSb, the spin moment of the Co at the surface increases to about 1.4 μ_B per Co atom while the spin moments of the Mn and Cr atoms in the subsurface layer slightly decrease due to the larger spin-down DOS around the Fermi level. Also, if one adds the spin moments for the surface and subsurface layers, the total spin magnetic moments are no longer almost integer moments due to the loss of the nearly half-metallicity. Ambrose *et al* [31] measured a spin magnetic moment of 5.1 μ_B for a Co_2MnGe thin film. This value is larger than the bulk value, in agreement with our results, but there is no experimental information on the characterization of the surface of the sample.

4.2. MnGe- and CrAl-terminated surfaces

In the case of the MnGe-terminated Co_2MnGe (001) surface the behaviour is similar to that for the MnSb-terminated surface in the CoMnSb compound. Due to the reduced symmetry (Mn loses two out of the four Co nearest neighbours), the hybridization between the Mn minority d states and the Co ones is reduced, leading to an increase of the Mn spin moment by about 0.6 μ_B, while the Co atom at the subsurface layer behaves similarly to in the bulk case. Where the Mn pseudogap was located in the bulk, there is now a small peak due to a d-like Mn atomic state that is shifted in energy due to the lower symmetry and which is pinned at the Fermi level. This state, although located at the surface layer, is not well localized and the Co atoms in the subsurface layer present a similar peak at the Fermi level. Ishida *et al* [40] have studied the MnSi- and MnGe-terminated Co_2MnSi and Co_2MnGe surfaces using a 13-layer-thick film. They claim that in the case of the MnSi surface the half-ferromagnetic character,

Table 4. As table 2, but for the MnGe- and CrAl-terminated (001) surfaces of the Co_2MnGe and Co_2CrAl compounds, respectively.

	Co_2MnGe	Co_2CrAl
Mn–Cr (↑/↓)	0.26/0.30	1.48/0.03
Ge–Al (↑/↓)	0.22/0.18	0.01/0.15
Co (↑/↓)	0.41/0.48	1.03/0.06
P_1 ($\frac{\uparrow-\downarrow}{\uparrow+\downarrow}$)	0%	78%
P_2 ($\frac{\uparrow-\downarrow}{\uparrow+\downarrow}$)	−6%	84%

which they have calculated for the bulk Co_2MnSi [29], is preserved, while in the case of the MnGe surface, surface states destroy the gap (in their paper they present results for the MnSi surface and only briefly refer to the MnGe surface). These results are peculiar, since they get a similar electronic structure for the bulk compounds and there is no obvious reason obliging only the MnGe surface to present surface states. Mn atoms have the same environment in both cases and the hybridizations between Mn and the sp atoms are similar for both Ge and Si. A plausible reason for this behaviour is the use of the atomic sphere approximation in their calculations, where the potential and the charge density are supposed to be spherically symmetric. Although this approximation can accurately describe the bulk compounds due to the close-packed structure they adopt, it is not suitable for surfaces where the non-spherical contributions to the potential and the charge density are important.

The case of Co_2CrAl is different from Co_2MnGe. In line with the reduction of the total number of valence electrons by 2, the Cr moment is rather small (1.54 μ_B) yielding a total moment of only 3 μ_B instead of 5 μ_B for Co_2MnGe. The Co-terminated $Co_2CrAl(001)$ surface shows a similar behaviour to the corresponding surface of Co_2MnGe, being in both cases dominated by a strong Co peak in the gap region of the minority band. However, the CrAl-terminated Co_2CrAl surface behaves very differently, being driven by the large surface enhancement of the Cr moment from 1.54 to 3.12 μ_B. As a consequence the splitting of the Cr peaks in the majority and minority bands is even enlarged and in particular in the minority band the pseudogap is preserved. Thus this surface is a rare case, since for all the other surfaces studied in this paper, the half-metallicity is destroyed by surface states.

4.3. Spin polarization

In the last part of my study I will discuss the spin polarization for the surfaces of the full-Heusler alloys. I will concentrate on the MnGe- and CrAl-terminated surfaces as the Co-terminated ones might show large reconstructions and thus are not interesting for applications. In table 4 I present the atom-resolved spin-up and spin-down DOS at the Fermi level and the spin polarization obtained. In the case of the MnGe-terminated surface the surface states completely kill the spin polarization as the majority-spin DOS is pretty small. In the case of the CrAl-terminated surface the situation is completely different. The minority DOS around the Fermi level is the same for both the bulk and the CrAl surface. The Fermi level falls within a region of very high Cr and Co majority-spin DOS, as can be seen in table 4, and thus 92% of the electrons at the Fermi level are of spin-up character and P_2 reaches 84%.

5. Summary

I have performed *ab initio* calculations based on the full-potential version of the screened KKR Green function method for the (001) surfaces of a series of half-ferromagnetic Heusler

alloys, i.e. for the half-Heusler alloys NiMnSb, CoMnSb and PtMnSb with the $C1_b$ structure and the full-Heusler alloys Co_2MnGe, Co_2MnSi and Co_2CrAl with the $L2_1$ structure. In the calculations the relaxation of the surfaces was not taken into account and this could change some of the details of the results. However, as was shown in [24], this effect at least for the MnSb-terminated surfaces is negligible. For the half-Heusler alloys, the MnSb-terminated (001) surfaces present electronic and magnetic properties similar to those of the bulk compounds. There is however a small finite Mn d and Sb p DOS within the bulk spin-down gap and these surface states are strongly localized at the surface layer. The spin polarization at the Fermi level for this termination reaches 38%. The (001) surfaces terminated at Ni, Co or Pt present a quite large density of states at the Fermi level and properties considerably different from those of the bulk and the MnSb-terminated surfaces. In the case of the Co-based full-Heusler alloys, the Co-terminated surfaces show a behaviour similar to that of the Co-terminated CoMnSb surface and the Co minority states shift in a practically rigid way towards higher energies, destroying the pseudogap. In the case of the MnGe-terminated $Co_2MnGe(001)$ surfaces, the surface states kill the spin polarization completely but in the case of CrAl the combination of the very high majority-spin Cr and Co DOS and the absence of surface states within the pseudogap result in a very high spin polarization of around 84%. Thus, of all the surfaces investigated, this is the only one which preserves the nearly half-metallicity at the surface.

Acknowledgments

The author acknowledges financial support from the RT Network of *Computational Magnetoelectronics* (contract RTN1-1999-00145) of the European Commission. The author would also like to thank Professor P H Dederichs for helpful discussions and for a critical reading of the manuscript.

References

[1] Baibich M N, Broto J M, Fert A, Nguyen Van Dau F, Petroff F, Etienne P, Creuzet G, Friederich A and Chazelas J 1988 *Phys. Rev. Lett.* **61** 2472
[2] Binasch G, Grünberg P, Saurenbach F and Zinn W 1989 *Phys. Rev.* B **39** 4828
[3] Kilian K A and Victora R H 2000 *J. Appl. Phys.* **87** 7064
Kilian K A and Victora R H 2001 *IEEE Trans. Magn.* **37** 1976
[4] Tanaka C T, Nowak J and Moodera J S 1999 *J. Appl. Phys.* **86** 6239
[5] Caballero J A, Park Y D, Childress J R, Bass J, Chiang W-C, Reilly A C, Pratt W P Jr and Petroff F 1998 *J. Vac. Sci. Technol.* A **16** 1801
Hordequin C, Nozières J P and Pierre J 1998 *J. Magn. Magn. Mater.* **183** 225
[6] Webster P J and Ziebeck K R A 1988 *Landolt–Börnstein New Series* Group III, vol 19c, ed H R J Wijn (Berlin: Springer) pp 75–184
[7] de Groot R A, Mueller F M, van Engen P G and Buschow K H J 1983 *Phys. Rev. Lett.* **50** 2024
[8] Galanakis I, Ostanin S, Alouani M, Dreyssé H and Wills J M 2000 *Phys. Rev.* B **61** 4093
[9] Youn S J and Min B I 1995 *Phys. Rev.* B **51** 10 436
[10] Kübler J 1984 *Physica* B **127** 257
[11] Kirillova M N, Makhnev A A, Shreder E I, Dyakina V P and Gorina N B 1995 *Phys. Status Solidi* b **187** 231
[12] Hanssen K E H M and Mijnarends P E 1990 *Phys. Rev.* B **34** 5009
Hanssen K E H M, Mijnarends P E, Rabou L P L M and Buschow K H J 1990 *Phys. Rev.* B **42** 1533
[13] Bobo J F, Johnson R J, Kautzky M, Mancoff F B, Tuncel E, Whit R L and Clemens B M 1997 *J. Appl. Phys.* **81** 4164
[14] van Roy W, de Boeck J, Brijs B and Borghs G 2000 *Appl. Phys. Lett.* **77** 4190
van Roy W, Borghs G and de Boeck J 2001 *J. Cryst. Growth* **227–8** 862
Schlomka J-P, Press W, Fitzsimmons M R, Lütt M and Grigorov I 1998 *Physica* B **248** 140
Schlomka J-P, Tolan M and Press W 2000 *Appl. Phys. Lett.* **76** 2005
[15] Soulen R J Jr *et al* 1998 *Science* **282** 85

[16] Mancoff F B, Clemens B M, Singley E J and Basov D N 1999 *Phys. Rev.* B **60** R12 565
[17] Zhu W, Sinkovic B, Vescovo E, Tanaka C and Moodera J S 2001 *Phys. Rev.* B **64** R060403
[18] Bona G L, Meier F, Taborelli M, Bucher E and Schmidt P H 1985 *Solid State Commun.* **56** 391
[19] Caballero J A, Reilly A C, Hao Y, Bass J, Pratt W P, Petroff F and Childress J R 1999 *J. Magn. Magn. Mater.* **198–9** 55
Kabani R, Terada M, Roshko A and Moodera J S 1990 *J. Appl. Phys.* **67** 4898
[20] Tanaka C T, Nowak J and Moodera J S 1997 *J. Appl. Phys.* **81** 5515
[21] Ristoiu D, Nozières J P, Borca C N, Komesu T, Jeong H-K and Dowben P A 2000 *Europhys. Lett.* **49** 624
Ristoiu D, Nozières J P, Borca C N, Borca B and Dowben P A 2000 *Appl. Phys. Lett.* **76** 2349
Borca C N, Komesu T, Jeong H-K, Dowben P A, Ristoiu D, Hordequin Ch, Pierre J and Nozières J P 2000 *Appl. Phys. Lett.* **77** 88
[22] Borca C N, Komesu T, Jeong H-K, Dowben P A, Ristoiu D, Hordequin Ch, Nozières J P, Pierre J, Stadler Sh and Idzerda Y U 2001 *Phys. Rev.* B **64** 052409
[23] Wijs G A and de Groot R A 2001 *Phys. Rev.* B **64** R020402
[24] Jenkins S J and King D A 2001 *Surf. Sci.* **494** L793
[25] Jenkins S J and King D A 2002 *Surf. Sci.* **501** L185
[26] Pierre J, Skolozdra R V, Tobola J, Kaprzyk S, Hordequin C, Kouacou M A, Karla I, Currat R and Lelièvre-Berna E 1997 *J. Alloys Compounds* **262–3** 101
Tobola J and Pierre J 2000 *J. Alloys Compounds* **296** 243
[27] Kübler J, Williams A R and Sommers C B 1983 *Phys. Rev.* B **28** 1745
[28] Webster P J 1971 *J. Phys. Chem. Solids* **32** 1221
[29] Ishida S, Akazawa S, Kubo Y and Ishida J 1982 *J. Phys. F: Met. Phys.* **12** 1111
Ishida S, Fuji S, Kashiwagi S and Asano S 1995 *J. Phys. Soc. Japan* **64** 2152
[30] Brown P J, Neumann K U, Webster P J and Ziebeck K R A 2000 *J. Phys.: Condens. Matter* **12** 1827
[31] Ambrose T, Krebs J J and Prinz G A 2000 *Appl. Phys. Lett.* **76** 3280
Ambrose T, Krebs J J and Prinz G A 2000 *J. Appl. Phys.* **87** 5463
[32] Geiersbach U, Bergmann A and Westerholt K 2002 *J. Magn. Magn. Mater.* **240** 546
[33] Zeller R, Dederichs P H, Újfalussy B, Szunyogh L and Weinberger P 1995 *Phys. Rev.* B **52** 8807
[34] Papanikolaou N, Zeller R and Dederichs P H 2002 *J. Phys.: Condens. Matter* **14** 2799
[35] Vosko S H, Wilk L and Nusair N 1980 *Can. J. Phys.* **58** 1200
[36] Zeller R 1997 *Phys. Rev.* B **55** 9400
[37] Galanakis I, Dederichs P H and Papanikolaou N 2002 *Preprint* cond-mat/0203534
[38] Borca C N, Komesu T and Dowben P A 2002 *J. Electron Spectrosc. Relat. Phenom.* **122** 259
[39] Galanakis I, Dederichs P H and Papanikolaou N 2002 *Preprint* cond-mat/0205129
[40] Ishida S, Masaki T, Fujii S and Asano S 1998 *Physica* B **245** 1